# Formation of Micro Lead in Cylindrical Plunge Grinding

**Jannik Röttger, Matthias Baumann, Frank Bauer, Sebastian Barth, Thomas Bergs**

Lead, especially micro lead, on ground shaft sealing surfaces has been an ongoing issue in sealing technology for many years. Now that suitable lead measuring methods have finally been developed, the scientific focus has shifted from the measurement of lead and its influence on the sealing function to the formation of lead. Experimental investigations have been carried out to analyse the influence of the process parameters on the formation of micro lead during external cylindrical plunge grinding. The results show that micro lead occurs using industrial common parameters. The influence of the grinding tool specification, the dressing and the grinding parameters on the micro lead structures are described and discussed.

## 1 Introduction

Rotary shaft seals are widely used sealing components to seal rotating shafts. In combination with the fluid to be sealed and the shaft counterface they form a complex tribological system. In operation, a tribologically suitable shaft counterface is essential for the formation of a hydrodynamic lubricant film between the sealing edge and the shaft surface and thus also for a reliable and long-lasting sealing function [1]. External cylindrical plunge grinding is the preferred manufacturing process for sealing surfaces. Alternative shaft manufacturing processes, such like belt finishing, turning or rolling processes, have proven to be less suitable or even completely unsuitable for sealing, [2]. But even ground surfaces are not applicable without restrictions. When using ground surfaces, seal manufacturers and users in the industry have to deal with the topic "Shaft Lead". Lead refers to surface structures which, depending on the direction of shaft rotation, cause an axial fluid transport effect through the sealing contact and thus cause either leakage or a thermal damage to the sealing components due to a lack of lubricant in the contact zone, compare Figure 1. In this context, the term surface structures, refers to structures that are created by the interactions of the grinding wheel with the part when grinding the surface. If this anisotropic grinding structures have a deviating orientation compared to the shaft circumferential direction, the shaft acts like a conveying thread during operation and triggers the pumping effect [3].

The effect of shaft lead on the sealing function has been the subject of many scientific investigations. One of the first mentions of lead is [4] in 1954. In the article, the occurrence of a thread-like and axial periodic surface structure running around the entire circumference of a ground shaft is mentioned, which caused leakage during operation of rotary shaft seals. Such a surface structure is called macro lead today. In [5], the formation mechanisms of macro lead during plunge grinding have been investigated. The dressing spiral, which is created during the dressing of the grinding wheel is transferred to the component according to the process kinematics, thus forming the thread like surface structure. Optical and tactile measurement methods for macro lead using frequency based evaluation algorithms such like Fast-Fourier-Transform (FFT) were developed and presented under the model concept of an axial periodic surface structure in [6–9] and [10].

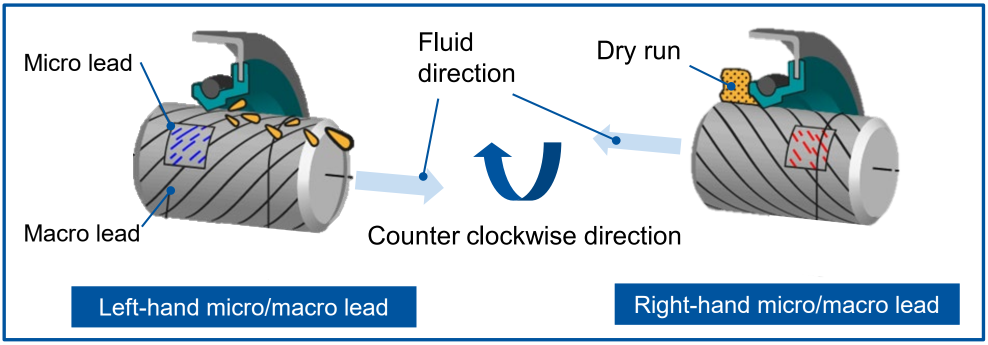


*Figure 1: Failure mechanisms due to lead structures*

Later it has been shown that not only macro lead is critical for sealing systems, [11]. The fine grinding grooves resulting from individual grain engagement during grinding can also have a direction deviating from the circumferential direction and thus also cause a pumping effect. Experiments showed, that the pumping effect of many fine grinding grooves can be even higher than the effect of macro lead structures. In this context, the term micro lead was introduced for the fine structures of ground surfaces. Since the previously existing measurement methods were unsuitable for detecting fine structures, a new approach for measuring micro lead was selected and developed in a series of research projects, [12–14]. An acquisition of ground surfaces with high-resolution optical topography measuring devices using a structure-based analysis with a statistical evaluation of the data, maps the stochastic characteristic of the grinding grooves in a targeted manner and thus has proven to be very functional. A further development of the approach has recently also been successfully applied to the evaluation of macro lead, [15, 16]. A graphical representation of both micro and macro lead is shown in Figure 2.

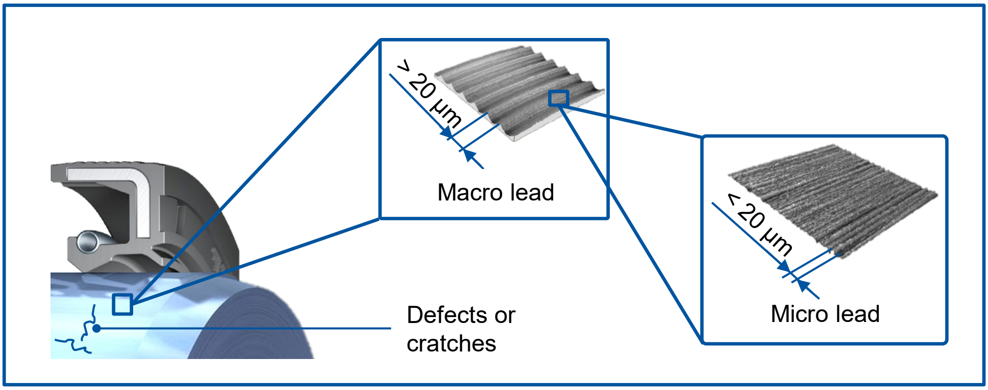


*Figure 2: Characteristics and scale of macro and micro lead on ground shaft sealing surfaces*

Experimental studies were conducted to investigate the pumping effect of micro and macro lead in sealing applications, [3, 17, 18]. For both macro and micro lead, the lead angle and the lead depth are decisive, with increasing pumping rate for increasing values of both parameters. In the case of macro lead, the axial period length of the lead structures also contributes to the height of the pumping effect as an additional parameter. The lower the axial period length, the more macro lead threads come into contact with the seal, resulting in a higher pumping rate. Especially period lengths of less than 0.15 mm are triggering a pumping effect. Also, it was found that the pumping effect of both macro and micro lead is directly linearly dependent on the shaft circumferential speed during sealing operation. And herein lies particularly the origin of increasing occurrence of lead-induced problems throughout the industry.

In the automotive industry, for example, the disruptive developments triggered by the demand for climate neutrality are constantly leading to higher performance requirements. Combustion engines are being replaced by electric drives, resulting in higher temperatures and more important in much higher sliding speeds in the electric powertrains. Shaft lead, which could previously be compensated for lower sliding speeds, now causes more often leakage in shaft sealing systems as the circumferential speeds increase continuously.

Apart from the fact that entangled axes of a grinding machine can cause micro lead, there have been no scientific publications dealing with the formation of micro lead, in contrast to the findings on the formation of macro lead. This is an essential lack of knowledge. To meet the future requirements, it will be important in the future to use sealing systems that are as optimally designed as possible, which requires the production of tribologically optimized shaft sealing surfaces. Therefore, experimental investigations have been carried out to analyse how and under which conditions micro lead occurs during external cylindrical plunge grinding. In these investigations the dressing and grinding parameters as well as the grinding wheel specification have been systematically varied. The ground surfaces have been evaluated by the IMA-MicroleadAnalysis. The identified correlations are the fundamentals for the knowledge-based grinding processes design for tribologically optimized shaft sealing surfaces with regard to micro-lead.

## 2 Materials and Methods

To investigate the correlations between the grinding and dressing parameters as well as the grinding tool specification on micro lead, grinding tests have been carried out at the LABORATORY FOR MACHINE TOOLS AND PRODUCTION ENGINEERING WZL OF RWTH AACHEN UNIVERSITY. The ground surfaces have been measured and evaluated at the INSTITUTE OF MACHINE COMPONENTS IMA OF STUTTGART UNIVERSITY. Following, the correlations have been analysed in close cooperation between both research institutes.

### 2.1 Experimental Setup

The external cylindrical plunge grinding investigations have been carried out using an external cylindrical grinding machine STUDER S41. A vitrified CBN grinding wheel (B126 VY200M TL of 3M) and a vitrified corundum grinding wheel (35A 80 I 8V 84 of KREBS & RIEDEL) have been used. Although the grinding wheels possess different grain sizes, they are used in industrial practice to achieve similar surface roughnesses. The selection of the grinding tools was done in close coordination with the grinding wheel manufacturers. Shaft workpieces (D 55 x 200 mm) made of hardened 100Cr6 (58±2HRC), a metal which is frequently used in power trains, have been ground in the experiments. The total depth of cut was $a_{e,tot} = 0.3\ mm$ per plunge cut. The number of spark out rotations to reduce the surface roughness without further infeed after roughing and finishing was $n_a = 3$. As dressing tool, a form roller with an active width of $b_s = 0.43\ mm$ (TESCH DIAMANTGESELLSCHAFT, diamond grainsize $d_k = 0.501\ mm$) was used.

Pre-experiments have been carried out to specify representative test parameters, which achieve surface roughnesses and macro geometries recommended for sealing systems. Based on this result, the central point of the design of experiments with the corundum wheel was set to a grinding wheel circumferential speed of $v_s = 40\ m/s$ and a radial feed rate of $v_{r,rough} = 1.5\ mm/min$ during roughing. This results in a specific material removal rate of $Q'_w = 4.20\ mm^3/mms$. After the roughing process, the radial feed rate was reduced to $v_{fr,fin} = 0.3\ mm/min$ which refers to a specific material removal rate of $Q'_w = 0.84\ mm^3/mms$. The total depth of cut during finishing was $a_{e,tot,fin} = 0.075\ mm$. The workpiece circumferential speed was $v_w = 0.4\ m/s$. This resulted in a grinding speed ratio between grinding wheel and workpiece of $q_s = 100$. As common for grinding between centers, up grinding was used. This means, that the velocity vectors of the grinding wheel and the workpiece in the contact point have different directions.

In the experimental investigations three test series have been carried out. In test series 1 the influence of the dressing parameters on the micro lead structures has been analysed for a corundum grinding wheel. In test series 2 a CBN grinding wheel has been applied. Based on the findings in test series 1 and 2, the influence of the grinding parameters on micro lead structures was in the focus of test series 3, where the CBN and the corundum grinding wheel have been used with constant dressing parameters for each grinding tool.

In the first series of tests, the dressing parameters for the corundum grinding wheel have been varied. The dressing overlap ratio $U_d$ and the ratio of dressing speeds have been varied according to the full factorial design of experiments shown in Figure 3. The dressing overlap ratio is the quotient of the active width of the dressing tool and the axial feed per grinding wheel revolution and was set to $U_d = 2.5, 4$ and $5.5$. The ratio of dressing speeds (form roller vs. grinding wheel circumferential speed) was $q_d = -0.5, 0.5$ and $0.8$. During the dressing process, the grinding wheel circumferential speed was $v_s = 40\, m/s$ and the depth of dressing cut was $a_{ed} = 15\,\mu m$. Before every grinding experiment, a pre-grinding process took place to ensure approximately constant wear conditions and grinding forces and thus reproducible test conditions. Constant engagement conditions have been tracked by grinding force measurement.

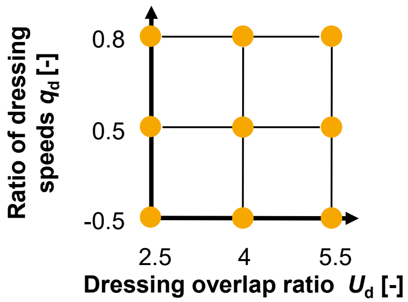


| Constant test parameters | Corundum |
|---|---|
| Grinding wheel circumferential speed $v_s$ | 40 m/s |
| Worpiece circumferential speed $v_w$ | 0.4 m/s |
| Specific material removal rate $Q'_w$ | 4.2 mm³/mms |
| Depth of dressing cut $a_{ed}$ | 15 µm |

*Figure 3: Grinding and dressing parameters for test series 1 with corundum*

To apply the CBN grinding wheel under industrial common conditions, the grinding wheel circumferential speed was set to $v_s = 80\, m/s$. To ensure the comparability with the corundum grinding wheel at the same time, the workpiece circumferential speed was set to $v_w = 0.8\, m/s$, which led to the same grinding speed ratio of $q_s = 100$. For the same reason, the radial feed rate was set to $v_{fr,rough} = 3\, mm/min$ ($v_{fr,fin} = 0.6\, mm/min$). The specific material removal rate during roughing was $Q'_w = 8.4\, mm^3/mms$ and $Q'_w = 1.4\, mm^3/mms$ during finishing. This resulted in the same equivalent chip thickness $h_{ec} = 0.1\,\mu m$ during roughing and $h_{ec} = 0.02\,\mu m$ during finishing as using the corundum grinding wheel. The equivalent chip thickness $h_{ec}$ is an approximate of the average thickness of the chips removed by one grinding grain, which depends on the process kinematics. Similar equivalent chip thicknesses $h_{ec}$ lead to comparable mechanical loads on each grain and chip formation mechanisms.

The design of experiments for CBN (Figure 4) was based on the investigations with the corundum grinding wheel. As pre-investigations showed, that the application of a CBN grinding wheel favoured the formation of micro lead, additional test points have been investigated. In addition, a dressing overlap ratio of $U_d$ = 8 has been used as well as ratios of dressing speeds of $q_d = -0.8, -0.3$ and $0.3$. As in the grinding process, the grinding wheel circumferential speed was $v_s = 80\ m/s$ during dressing and the depth of dressing cut was $a_{ed} = 2.5\ \mu\text{m}$, which is a common value for the dressing of superabrasive grain materials with higher hardness in comparison to corundum [26].

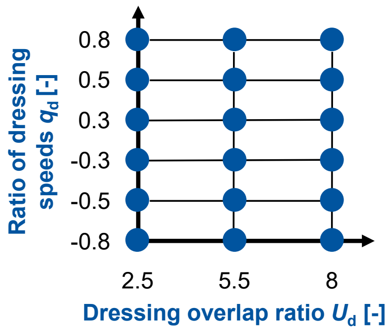


| Constant test parameters | CBN |
|---|---|
| Grinding wheel circumferential speed $v_s$ | 80 m/s |
| Worpiece circumferential speed $v_w$ | 0.8 m/s |
| Specific material removal rate $Q'_w$ | 8.4 mm³/mms |
| Depth of dressing cut $a_{ed}$ | 2.5 µm |

*Figure 4: Grinding and dressing parameters for test series 2 with CBN*

Based on the findings of the two test series, in test series 3 the influence of the grinding parameters for constant dressing parameters has been investigated. The radial feed rate $v_{fr}$, the spark out time $t_a$ and the grinding speed ratio $q_s$ have been varied according to the experimental design in Figure 5.

For both grinding wheels the grinding wheel circumferential speed was adjusted to achieve a grinding speed ratio of $q_s = 75, 100$ and $125$ while the workpiece circumferential speed remains constant. The radial feed rate was set to $v_{fr} = 1, 1.5$ and $2\ mm/min$ for the corundum grinding wheel and to $v_{fr} = 1, 2$ and $3\ mm/min$ for the CBN grinding wheel. Based on the findings two representative dressing parameter combinations have been chosen for each grinding wheel. To ensure that surface roughness was still in a range to be used for sealing counterfaces, the dressing overlap ratio for corundum has been increased to $U_d = 8$. An increase in the radial feed rate for CBN led to chatter marks and was not carried out. In addition, the spark out times have been varied according to the experimental design shown in Figure 5. As the results in test series 2 showed micro lead structures using the CBN grinding wheel, more parameter combinations have been investigated for the CBN grinding wheel to analyse the cause-effect-relations.

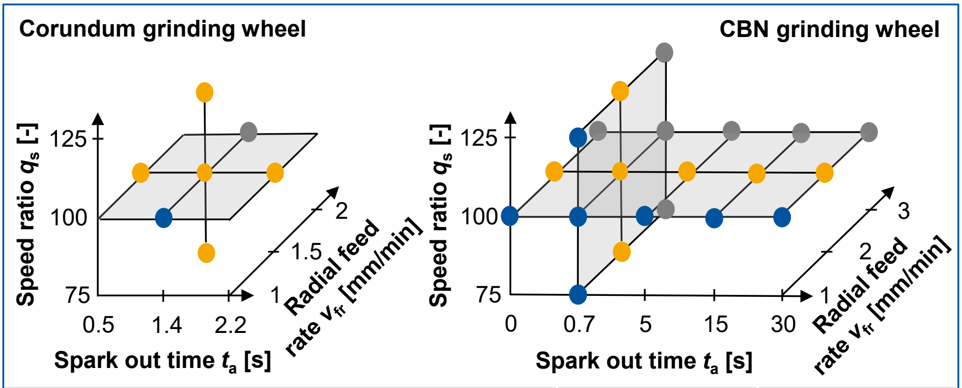


| Test parameters | Corundum | CBN |
|---|---|---|
| Ratio of dressing speeds $q_d$ | 0.5 | -0.5 |
| Dressing overlap ratio $Du$ | 8 | 5.5 |
| Workpiece circumferential speed $v_w$ | 0.4 | 0.8 |
| Depth of dressing cut $a_{ed}$ | 15 µm | 2.5 µm |

*Figure 5: Grinding parameter variation in test series 3*

## 2.2 Micro lead measurement

The IMA-MICROLEAD®ANALYSIS, shown in Figure 6, is a structure-based evaluation method for sealing surfaces, based on three-dimensional topographic surface data, measured by modern optically surface measurement instruments, such like confocal microscopes or white light interferometers (Figure 6.1). The method has already been presented several times in various stages of development at the “International Sealing Technology Conference” [19–23] before it was finally developed by the IMA to market maturity. The original development of a new approach was inspired by the lack of suitable methods for the measuring, analysis and description of microscopic lead structures.

In the context of a so-called structure-based surface analysis, a grinding structure is considered to be a single grinding groove resulting from the engagement of an abrasive grain. Instead of the common 2D and 3D surface parameters like $Rz, Ra, Sz$ or $Sa$, the method uses digital image processing algorithms, like segmentation (Figure 6.2) and feature extraction to separate and to analyse single grinding structures with regard to geometric properties (Figure 6.3). With this procedure, surface topographies are divided into structural elements that are evaluated individually. In this way, the angular orientation, the volume, the length, the width and the depth of each located single grinding structure are computed within an areal high-resolution measuring field, see Figure 6 (4.b). This resulting extensive set of data, containing geometrical properties of many grinding structures (Figure 6.4.a), are analysed by means of statistical methods (see Figure 6.4).

A component of such an evaluation is, for example the distribution curve $WV$ (Figure 6.4.c) of the computed angles of the structures. Closer inspection reveals, that there is normally no uniform preferred direction of the structure angles in the shaft circumferential direction. Many structures have slightly different orientations. The distribution corresponds to a Gaussian distribution. If the $WV$ curve shows an approximately symmetrical distribution with a maximum at an angle of 0°, which corresponds to the circumferential direction of the shaft, the measurement shows a micro-lead-free surface. When the curve results asymmetrically and shifted to either the positive or negative direction the measurement results in a micro lead afflicted surface. In addition to the distribution diagrams of the structure orientation (Figure 6.4.c) and the oriented structure volume (Figure 6.4.d), several derived micro lead parameters are also part of the evaluation. A complete overview of all parameters can be found in [3, 24].

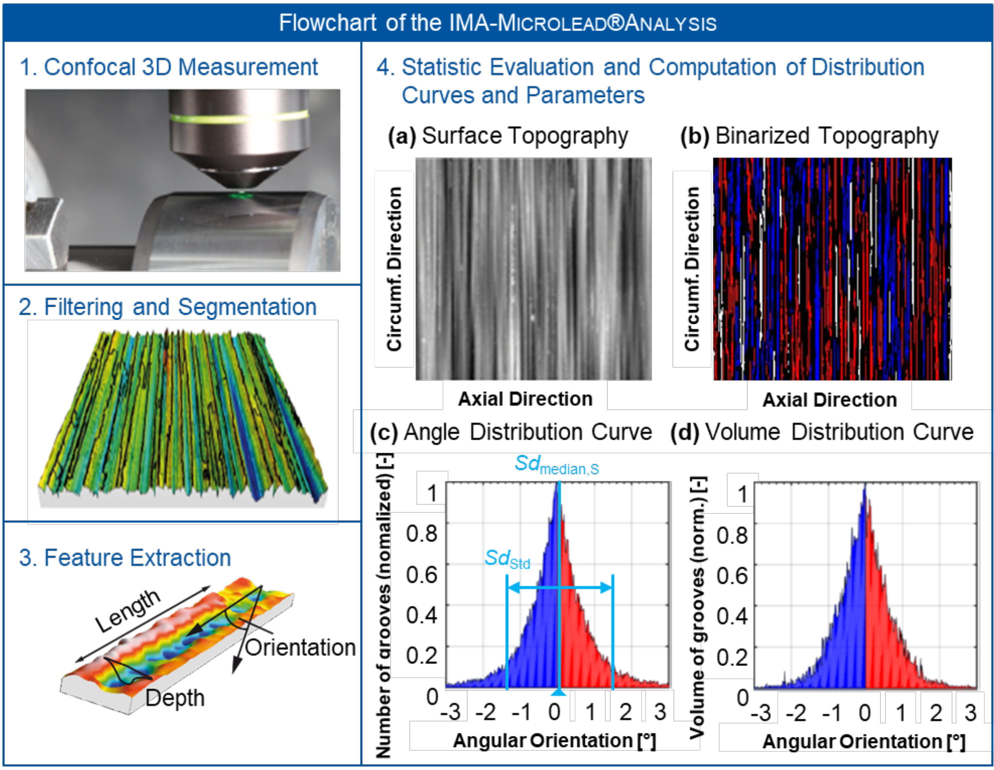


*Figure 6: Flowchart of the micro lead analysis*

For the consideration of the further results of the experiments carried out, two parameters of the IMA-MICROLEAD®ANALYSIS are mainly relevant. The median angle of the angular distribution $Sd_{median,S}$ is the median value of the angular orientation of all evaluated grinding structures.

$$Sd_{median,S} = median(WV(\gamma)) \tag{1}$$

The parameter directly indicates if the overall structure orientations deviate from the circumferential direction. It can be considered as the micro lead angle and should be 0° for micro lead free surfaces.

The standard deviation of the angular orientations $Sd_{std}$ represents the width of the angular distribution curve (4.c) and is specifically relevant, because broader angular distributions have proven to be less harmful for a sealing system.

$$Sd_{std} = std\big(WV(\gamma)\big) \tag{2}$$

In the case of a wider angular distribution, if the curve shifts in the positive or negative direction, the percentages of the positively or negatively directed structures change more slowly than in the case of narrow angular distributions. This therefore results in a more robust sealing system. Thus, one goal for achieving well suited surfaces for rotary sealings is to increase $Sd_{std}$ while reaching a value of $Sd_{median,S}$ = 0°.

## 3 Results

Figure 7 shows an overview of all investigated test points for the corundum and the CBN grinding wheel. The x-axis refers to the standard deviation of the angular orientations $Sd_{std}$, the y-axis refers to the median angle of the angular distribution $Sd_{median,S}$. Although industrial common process parameters have been used for both grinding wheels, which led to a similar range of surface roughness, it is noticeable, that the application of the CBN grinding wheel favours the formation of micro lead. A median angle of the angular orientations up to $Sd_{median,S} = -\ 0.14°$ occurred. Pre-investigations at IMA have shown, that micro lead angles in this range cause leakage during sealing operation with rotary shaft seals. On the same time, the surfaces ground with CBN show a higher range of the standard deviation of the angular orientations of $Sd_{std}$ = 0–1.7. Remarkable is the negative correlation between the standard deviation of angular orientations and the median angle of the micro lead structures. An increase of the standard deviation of the angular orientations $Sd_{std}$ leads to an increasing negative median angle of the angular distribution $Sd_{median,S}$ for CBN. Thus, a more detailed experimental design has been investigated for CBN.

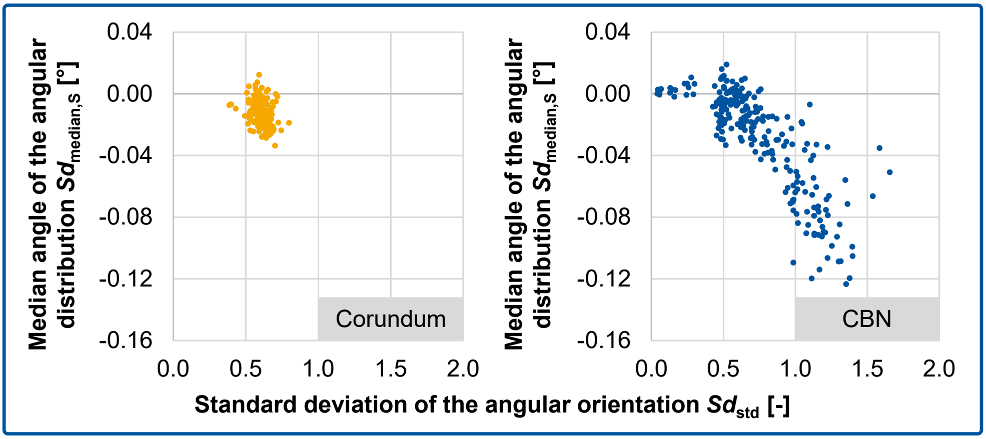


*Figure 7: Influence of the grinding wheel specification on micro lead formation*

The points in the following diagrams show the mean value of the three repetitions for each test point. Error bars indicate the range between the smallest and largest measured value for the test repetitions.

A detailed analysis of the correlations between the dressing parameters and the median angle of the angular distribution $Sd_{median,S}$ confirms the above-mentioned observations for the corundum grinding wheel, where less micro lead structures occurred in comparison with CBN. For corundum, no significant influence of the dressing overlap ratio $U_d$ or ratio of dressing speeds $q_d$ could be determined, see *Figure 8*. All $Sd_{median,S}$ values were between 0° and 0.03°, which can be regarded as micro lead free. The standard deviation of the angular orientations was between $Sd_{Std}$ = 0.4 and 0.8. Tendentially higher ratio of dressing speeds lead to smaller standard deviation of the angular orientations $Sd_{Std}$.

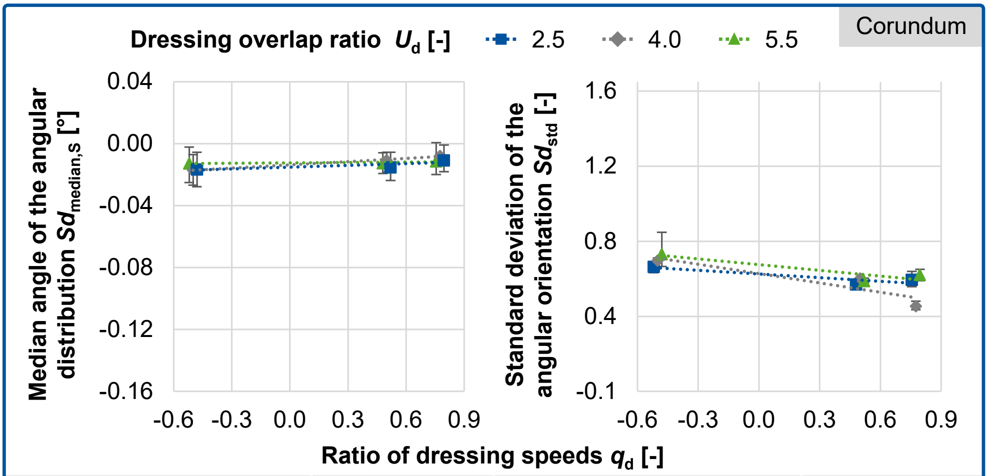


| | | | |
|---|---|---|---|
| Grinding wheel circumferential speed $v_s$ | 40 m/s | Specific material removal rate $Q'_w$ | 4.2 mm³/mms |
| Workpiece circumferential speed $v_w$ | 0.4 m/s | Depth of dressing cut $a_{ed}$ | 15 µm |

*Figure 8: Influence of the dressing parameters on the median angle of the angular distribution $Sd_{median,S}$ for corundum grinding wheel*

For the CBN grinding wheel, the lowest ratio of dressing speeds $q_d$ caused the most critical median angles of the angular distribution $Sd_{median,S}$ = 0.14°. The correlations are shown in Figure 9. For constant dressing overlap ratios $U_d$, an increase of the ratio of dressing speeds $q_d$ led to an increase in the median angle of the angular distribution up to $Sd_{median,S}$ = 0° (micro lead free). Furthermore, an increase in the dressing overlap ratio $U_d$ led to decreasing median angles of the angular distribution $Sd_{median,S}$. For the standard deviation of the angular orientations $Sd_{Std}$ contrary trends have been observed. Increasing ratios of dressing speed $q_d$ as well as decreasing dressing overlap ratios $U_d$ created lower median angles of the angular distribution $Sd_{median,S}$.

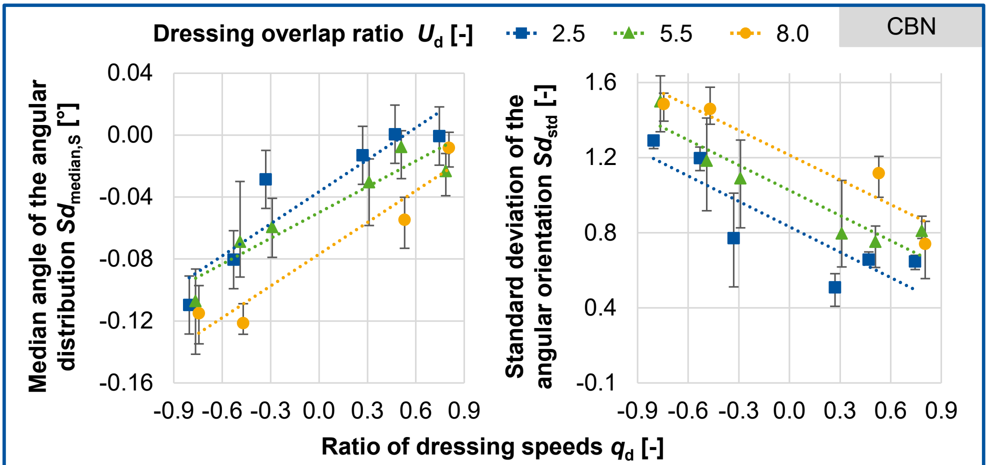


| | | | |
|---|---|---|---|
| Grinding wheel circumferential speed $v_s$ | 80 m/s | Specific material removal rate $Q'_w$ | 8.4 mm³/mms |
| Workpiece circumferential speed $v_w$ | 0.8 m/s | Depth of dressing cut $a_{ed}$ | 2.5 µm |

*Figure 9: Influence of the dressing parameters on the median angle of the angular distribution $Sd_{median,S}$ for CBN grinding wheel*

In further investigations, the influence of the grinding parameters for constant dressing parameters has been analysed. For the corundum grinding wheel similar trends compared to the dressing parameter influences have been observed. It was not possible to identify significant changes of the median angle of the angular distribution $Sd_{median,S}$ in dependence of the spark out time $t_a$, the grinding wheel circumferential speed $v_s$ or the radial feed rate $v_{fr}$, see Figure 10. The standard deviation of the angular orientation $Sd_{Std}$ showed an increase for increasing grinding wheel circumferential speeds $v_s$.

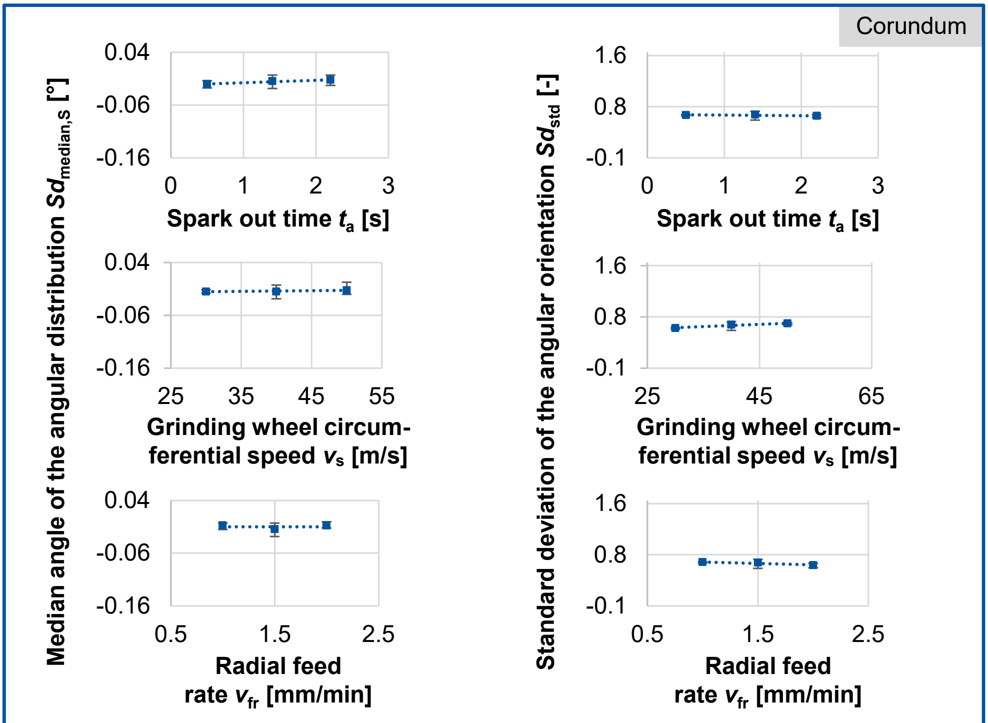


| | | | |
|---|---|---|---|
| Workpiece circumferential speed $v_w$ | 0.8 m/s | Depth of dressing cut $a_{ed}$ | 15 µm |
| Dressing overlap ratio $U_d$ | 8 | Ratio of dressing speeds $q_d$ | 0.5 |

*Figure 10: Influence of the grinding parameters on lead structures for corundum grinding wheel*

For the investigations of the influence of the grinding parameters on micro lead with the CBN grinding wheel, one dressing parameter setting has been chosen, which produced significant lead structures in the dressing test. An increase in the grinding wheel circumferential speed $v_s$ resulted in a reduction of the median angle of the angular distribution $Sd_{median,S}$ for a radial feed rate $v_{fr}$ = 1 mm/min and 2 mm/min. For the highest investigated radial feed rate $v_{fr}$ = 3 mm/min, the increase in the grinding wheel circumferential speed did not affect the median angle of the angular distribution $Sd_{median,S}$.

For all investigated radial feed rates $v_{fr}$, an increase in the grinding wheel circumferential speed $v_s$ led to a reduction of the standard deviation of the angular orientation $Sd_{Std}$. The correlations are shown in Figure 11.

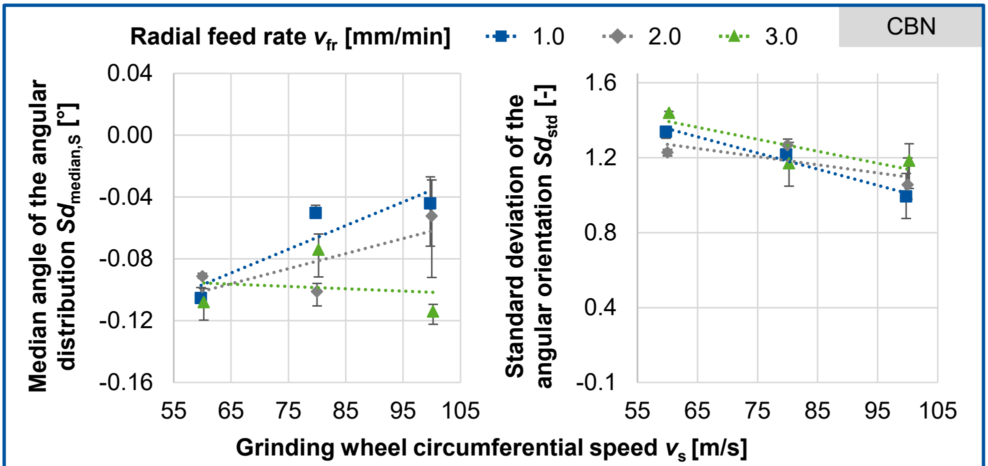


| | | | |
|---|---|---|---|
| Spark out time $t_a$ | 0.7 s | Specific material removal rate $Q'_w$ | 8.4 mm³/mms |
| Workpiece circumferential speed $v_w$ | 0.8 m/s | Depth of dressing cut $a_{ed}$ | 2.5 µm |
| Dressing overlap ratio $U_d$ | 5.5 | Ratio of dressing speeds $q_d$ | -0.5 |

*Figure 11: Influence of the grinding wheel circumferential speed vs on micro lead structures for CBN grinding wheel*

Figure 12 shows the influence of the spark out time $t_a$ on the resulting micro lead structures. For all investigated radial feed rates $v_{fr}$, highly negative median angles of the angular distribution $Sd_{median,S}$ occurred for grinding with short spark out time $t_a$. An increase in the spark out time from $t_a$ = 15 to $t_a$ = 30 s did not result in a further increase of the median angles of the angular distribution $Sd_{median,S}$. With regard to the standard deviation of the angular orientation $Sd_{Std}$ a negative correlation was identified, especially for a radial feed rate of $v_{fr}$ = 2 mm/min.

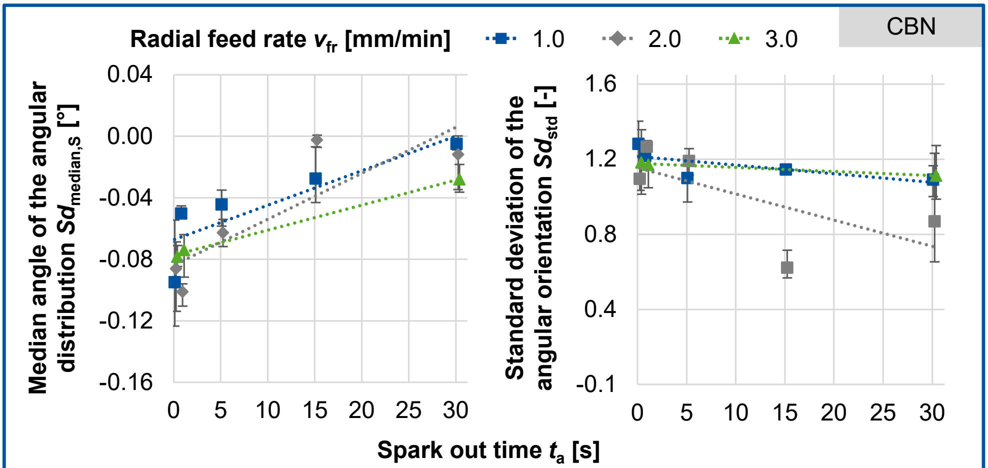


| | | | |
|---|---|---|---|
| Grinding wheel circumferential speed $v_s$ | 80 m/s | Specific material removal rate $Q'_w$ | 8.4 mm³/mms |
| Workpiece circumferential speed $v_w$ | 0.8 m/s | Depth of dressing cut $a_{ed}$ | 2.5 µm |
| Dressing overlap ratio $U_d$ | 5.5 | Ratio of dressing speeds $q_d$ | -0.5 |

*Figure 12: Influence of the spark out time $t_a$ on micro lead structures for CBN grinding wheel*

## 4 Discussion

Although comparable engagement situations for the CBN and the corundum grinding wheel were present, the application of a corundum grinding wheel shows a better suitability for the manufacturing of radial sealing counterfaces. Although a wide range of industrial common grinding and dressing parameters has been investigated, no functional critical lead structures have been identified.

Possible reasons can be the splittering behaviour of the corundum grains, which are dressed with higher depths of dressing cut. This leads to a higher degree of grain breakout and can cause an unregular grinding wheel topography which does not create inclined structures on the workpiece. As corundum grains wear more than superabrasives, the grinding wheel topography is changing during operation because of changes in grain geometry and self-sharpening effects, where blunt grains break out and new sharp grains come in contact with the workpiece. This can also prevent the formation of inclined structures on the workpiece.

CBN grinding wheels are dressed with a smaller depth of cut because of their higher hardness. Aggressive dressing parameters, e. g. high ratios of dressing speed $q_d$ and small dressing overlap ratios $U_d$, which tend to create a rough grinding wheel topography, showed the best suitability for grinding micro lead free radial shaft sealing counterfaces.

A negative ratio of dressing speeds tends to a long engagement path between dressing tool and grinding wheel in comparison to positive ratio of dressing speeds, [25]. If this rotation is superposed with the axial dressing feed, inclined structures on the grinding wheel surface are created. In dependence of the ratio of rotational speeds between grinding wheel and workpiece they can be reproduced skewedly at the ground surface and produce micro lead structures with critical median angles of the angular distribution $Sd_{median,S}$. An increase of the ratio of dressing speeds $q_d$ led to an increase in the median angle of the angular distribution up to $Sd_{median,S}$ = 0° (micro lead free).

Furthermore, an increase in the dressing overlap ratio $U_d$ led to decreasing median angles of the angular distribution $Sd_{median,S}$, which can cause leakage. Because of the smaller axial dressing feed rate, a smaller CBN volume is dressed per grinding wheel revolution. According to LINKE, this causes a micro grain breakage at the grain peaks, [25]. Opposite to this, small dressing overlaps and high axial dressing feed rates lead to a high dressing chip diameter, [25]. This provokes a higher degree of grain macro grain breakage or breakout of complete grains which results in an undefined grinding wheel topography without systematic structures, that can be reproduced on the workpiece surface. Although it would be obvious, that high axial feed rates increase the micro lead angle, the engagement kinematics lead to grain breakouts and irregular splittering of the CBN grains which helps to avoid inclined micro structures.

Tendentially higher ratios of dressing speeds $q_d$ led to a smaller standard deviation of the angular orientations $Sd_{Std}$. A higher ratio of dressing speeds $q_d$ leads to a higher roughness of the grinding wheel with a high grain protrusion. Thus, a smaller number of grains comes in contact with the workpiece and creates a smaller number of grinding grooves, [25]. They possess a lower deviation of the angular orientation.

An increase in the dressing overlap ratio $U_d$ leads to a fine grinding wheel topography with a large number of cutting edges with low grain protrusion, [26]. Every cutting edge has its individual geometry. The workpiece material is machined by a higher number of grain engagements. This results in a higher number of grinding structures on the ground surface, that are a result of the grain geometry. Thus, a higher standard deviation of angular orientation $Sd_{Std}$ can be observed.

An increase in the grinding wheel circumferential speed $v_s$ for constant specific material removal rates $Q'_w$ means that the same workpiece material is machined by more grain engagements. This results in more grinding structures on the surface, which can have a higher standard deviation.

Furthermore, an increase in the radial feed rate $v_{fr}$ leads to higher chip thicknesses a lower number of grain engagements and thus to larger grinding grooves with smaller deviation.

An increase in the grinding wheel circumferential speed $v_s$ leads to smaller chip thicknesses. One explanatory approach, that ca be derived is, that the forces on each grain are reduced which can also reduce their deflection. A smaller standard deviation of angular orientation $Sd_{Std}$ is the result, because without grain deflection the grain orientation is more similar.

An increase in the spark out time $t_a$ resulted tendentially in median angles $Sd_{median,S}$ closer to 0° and with lower deviation from the circumferential orientation. A possible hypothesis for this behaviour is the decreasing contact lengths because of the reduction of the infeed.

As the application of CBN grinding wheels is used for the economical production of large batch sizes with reduced grinding wheel wear, they cannot be replaced by corundum grinding wheels without disadvantages. CBN grinding wheels allow higher grinding wheel circumferential speeds and specific material removal rates. Because of the higher thermal conductivity of CBN in comparison with corundum, the risk of grinding burn is shifted to higher machining rates. These facts allow a higher productivity. The hardness of CBN reduces grinding wheel wear, which increases the possible batch sizes and reduces the dressing efforts. This has a positive influence on the process reliability, [26]. Thus, a knowledge-based process design is necessary to profit of the positive application behaviour of CBN in the production of radial sealing counterfaces. A high standard deviation of the angular orientation $Sd_{Std}$ led to increasing negative median angles of the angular distribution $Sd_{median,S}$. For tribologically optimized sealing counterfaces median angles of the angular distribution of $Sd_{median,S} = 0°$ and a high standard deviation of the angular orientation $Sd_{Std}$ are the objective. As the results showed that a high standard deviation occurred in combination with high micro lead angels, a target conflict has to be solved.

Further investigation will focus on a fundamental understanding of the formation of inclined micro structures in the single grain contact. A FE-model will help to analyse the influence of the grain geometry on the micro lead structures. The correlations between grain geometry and micro lead will be transferred to the multi grain engagement by measuring the grinding wheel topography in dependence of the dressing parameters.

## 5 Summary and Conclusion

In order to achieve functional and reliable sealing systems with rotary shaft seals, a suitable lead-free shaft sealing surface is required. First, the problems were described why the issue of lead has caused problems in the industry for many years and why the problems are still increasing although lead measurement methods are now available. The trend towards higher requirements on system components will certainly continue. A knowledge-based design of the manufacturing processes used for the manufacturing of the components will thus become inevitable. First essential steps towards a knowledge-based design of external cylindrical plunge grinding processes for tribologically suitable sealing surfaces were presented in this article. In experimental investigations at the LABORATORY FOR MACHINE TOOLS AND PRODUCTION ENGINEERING WZL OF RWTH AACHEN UNIVERSITY, the dressing and grinding parameters have been varied and the ground surface were measured by IMA-MicroleadAnalysis at the INSTITUTE FOR MACHINE ELEMENTS IMA AT STUTTGART UNIVERSITY.

In general, a corundum grinding wheel showed a better application for the grinding of lead free surfaces, since only small lead angles close to the circumferential direction of the shafts resulted. No influence of any grinding or dressing parameters on the resulting micro lead angle could be determined.

In contrast to this, a CBN grinding wheel in combination with a highly negative ratio of dressing speeds and a high dressing overlap ratios repeatably produced functional critical micro lead structures, although an industrial common range of parameter has been used. This means that under certain circumstances, lead afflicted shaft surfaces can enter the market in batches without the knowledge of those responsible. This can have significant economic consequences for companies and underlines the need for appropriate quality control.

## 6 Literaturverzeichnis:

[1] **Bauer, F.:** *Federvorgespannte-Elastomer-Radial-Wellendichtungen. Grundlagen der Tribologie & Dichtungstechnik, Funktion und Schadensanalyse*, Wiesbaden, Heidelberg: Springer Vieweg, 2021, Springer Fachmedien Wiesbaden, - ISBN 978-3-658-32921-1.

[2] **Schulz, M.; Baumann, M.; Bauer, F.:** *Influence of different shaft surface finishes on the lubrication and friction condition of elastomeric lip seals.* 7th International Conference Integrity-Reliability-Failure, Funchal/ Portugal, 6-10 September 2020, 2020, S. 351–368 - ISBN 978-989-54756-1-2.

[3] **Baumann, M.:** *Abdichtung drallbehafteter Dichtungsgegenlaufflächen - Messung, Analyse, Bewertung und Grenzen*. Dissertation, 2017, Universität Stuttgart, Institut für Maschinenelemente, - ISBN 978-3-936100-69-3.

[4] **Lein, J.:** *Mechanische Untersuchungen an Dichtungsringen für rotierende Wellen*, Berlin, Heidelberg: Springer Verlag, 1954, - ISBN 3662253356.

[5] **Kersten, G.:** *Optische und antastende Prüfung der Gegenlauffläche von Radial-Wellendichtringen*, Düsseldorf: VDI Verlag, 1992, Verein Deutscher Ingenieure e.V. (VDI), - ISBN 3-18-148102-5.

[6] **Seewig, J.; Hercke, T.:** *2nd Generation Lead Measurement.* XIX IMEKO World Congress, Lisbon, Portugal, September 6-11, 2009, 2009 - ISBN 9781615675937.

[7] **Rau, N.; Seibold, M.:** *Drallstrukturen an geschliffenen Dichtflächen und ihr Einfluss auf die Dichtfunktion.* 11th International Sealing Conference, Dresden, 03./04. Mai 1999, 1999, S. 393–404.

[8] **Beyerer, J.:** *Analyse von Riefentexturen*, Düsseldorf: VDI-Verlag, 1994, Verein Deutscher Ingenieure e.V. (VDI), - ISBN 3-18-339008-6.

[9] **Puente León, F.:** *Drallerkennung an Gegenlaufflächen von Radialwellendichtringen.* Bildverarbeitung im industriellen Einsatz, Stuttgart, 18./19.10.2000; VDI-Berichte; Düsseldorf: VDI-Verlag, 2000, S. 117–122.

[10] **Hertzsch, A.; Kröger, K.; Großmann, M.:** *Schnelle optische Drallmessung*. tm – Technisches Messen. 2013, 80 (12).

[11] **Kunstfeld, T.:** *Einfluss der Wellenoberfläche auf das Dichtverhalten von Radial-Wellendichtungen*. Dissertation, 2005, Universität Stuttgart, Institut für Maschinenelemente, - ISBN 3-936100-16-0.

[12] **Baitinger, G.; Haas, W.:** *Strukturanalyse. Drall- und Mikrostrukturanalyse zur funktionalen Bewertung von Dichtringgegenlaufflächen*. Abschlussbericht FKM Vorhaben Nr. 285, AiF-Nr. 15628 N/1, Frankfurt am Main: FKM, 2011, Forschungskuratorium Maschinenbau e.V. (FKM).

[13] **Baumann, M.; Bauer, F.; Haas, W.:** *Strukturanalyse II. Ganzheitliche, funktionale Bewertung von Dichtungsgegenlaufflächen mittels Strukturanalyse unter Einbeziehung der Wirkung von Strukturen auf die Förderwirkung der Welle*. Abschlussbericht FKM Vorhaben Nr. 298, IGF-Nr. 17138 N/1, Frankfurt am Main: FKM, 2015, Forschungskuratorium Maschinenbau e.V. (FKM).

[14] **Baumann, M.; Bauer, F.:** *Strukturanalyse III. Anwendung von Strukturanalyse und Festlegung von Qualitätskriterien für die gezielte Bewertung von Dichtungsgegenlaufflächen*. Abschlussbericht FKM Vorhaben Nr. 308, IGF-Nr. 18186 N, Frankfurt am Main: FKM, 2017, Forschungskuratorium Maschinenbau e.V. (FKM).

[15] **Engelfried, M.; Baumann, M.; Bauer, F.:** *3D-Makrodrall - Strukturbasierte 3D-Analyse von Makrodrall*. Forschungsheft 1471, Forschungsvereinigung Antriebstechnik e.V., Abschlussbericht FVA Vorhaben Nr. 876 I, Frankfurt am Main, 2022.

[16] **Engelfried, M.; Baumann, M.; Bauer, F.:** *Three-dimensional structure-based approach for the analysis of macroscopic lead structures on sealing counterfaces*. International Journal of Metrology and Quality Engineering. 2022, 13-2/2022 , S. 1–14.

[17] **Schiefer, F.; Baumann, M.; Bauer, F.:** *Untersuchung des Förderverhaltens makrodrall-behafteter Dichtungsgegenlaufflächen.* 20th International Sealing Conference (ISC), Stuttgart, 10.-11. Oktober 2018; Fluidtechnik; Frankfurt am Main: Fachverband Fluidtechnik im VDMA e.V, 2018, S. 301–312 - ISBN 978-3-8163-0727-3.

[18] **Schiefer, F.; Matus, M.; Bauer, F.; Poll, G.:** *Schädliche Strukturen (Drall). Erkennen und Bewerten von schädlichen Strukturen auf RWDR-Gegenlaufflächen*. Abschlussbericht FVA-Vorhaben Nr. 805 I, Frankfurt am Main: FVA, 2020, Forschungsvereinigung Antriebstechnik e.V. (FVA).

[19] **Baumann, M.; Bauer, F.:** *Moderne visuelle Untersuchungsmethoden für die Verschleißanalyse am Beispiel Radial-Wellendichtring.* 20th International Sealing Conference (ISC), Stuttgart, 10.-11. Oktober 2018; Fluidtechnik; Frankfurt am Main: Fachverband Fluidtechnik im VDMA e.V, 2018, S. 93–104 - ISBN 978-3-8163-0727-3.

[20] **Baumann, M.; Bauer, F.; Haas, W.:** *Empirische Modellierung der Drall-induzierten Fluidförderwirkung von Dichtungsgegenlaufflächen – Sind Grenzen möglich?* 19th International Sealing Conference (ISC), Stuttgart, 12.-13. Oktober 2016; Fluidtechnik; Frankfurt am Main: Fachverband Fluidtechnik im VDMA e.V, 2016, S. 110–121 - ISBN 978-3-8163-0684-9.

[21] **Baitinger, G.:** *Multiskalenansatz mit Mikrostrukturanalyse zur Drallbeurteilung von Dichtungsgegenlaufflächen*. Dissertation, 2011, Universität Stuttgart, Institut für Maschinenelemente, - ISBN 978-3-936100-36-5.

[22] **Baitinger, G.; Haas, W.:** *Ganzheitlicher Ansatz zur Charakterisierung der Topologie von Dichtungslaufflächen.* 15th International Sealing Conference (ISC), Stuttgart, Germany, October 7 - 8, 2008; Ebelsbach: Leithner Media Production, 2008, S. 97–108 - ISBN 3-00025-884-1.

[23] **Baitinger, G.; Haas, W.:** *Drallmessung mittels Mikrostrukturanalyse.* 16th International Sealing Conference (ISC), Stuttgart, 12./13.10.2010; Ebelsbach: Leithner Media Production, 2010, S. 341–350 - ISBN 3-00032-523-9.

[24] **Universität Stuttgart, Institut für Maschinenelemente:** *IMA-Mikrodrall®Analyse.* Universität Stuttgart, Institut für Maschinenelemente (Hrsg.), IMA-TechSheet, V1, #104140, Stuttgart, URL: https://www.ima.uni-stuttgart.de/dokumente/forschung/dichtungstechnik/dienstleistungen/104140.pdf.

[25] **Linke, B. S.:** *Wirkmechanismen beim Abrichten keramisch gebundener Schleifscheiben*. Zugl.: Aachen, Techn. Hochsch., Diss., 2007, Aachen: Shaker, 2007, - ISBN 9783832265731.

[26] **Klocke, F.:** *Fertigungsverfahren 2. Zerspanung mit geometrisch unbestimmter Schneide,* 5. Aufl. 2017, Berlin, Heidelberg: Springer Berlin Heidelberg, 2017, - ISBN 978-3-662-53309-3.

## 7 Authors

**University of Stuttgart, Institute of Machine Components (IMA)**

**Pfaffenwaldring 9, 70569 Stuttgart, Germany:**

Dr.-Ing. Matthias Baumann, ORCID 0000-0002-1962-5153, matthias.baumann@ima.uni-stuttgart.de

PD. Dr.-Ing. Frank Bauer, ORCID 0000-0001-7799-7628, frank.bauer@ima.uni-stuttgart.de

**RWTH Aachen University, Laboratory for Machine Tools and Production Engineering (WZL)**

**Campus-Boulevard 30, 52074 Aachen, Germany:**

Jannik Röttger, M. Sc., ORCID 0000-0002-0163-9581, j.roettger@wzl.rwth-aachen.de

Dr.-Ing. Sebastian Barth, ORCID 0000-0002-0586-3839, s.barth@wzl.rwth-aachen.de

Prof. Dr.-Ing. Thomas Bergs, ORCID 0000-0003-2754-2689, t.bergs@wzl.rwth-aachen.de